Enhanced ballistic phonon production for surface events in cryogenic silicon detector

R.M. Clarke, P.L. Brink, B. Cabrera, P. Colling, M.B. Crisler[b)], A.K. Davies,
S. Eichblatt[b)], R.J. Gaitskell[a)], J. Hellmig[a)], J.M. Martinis[d)], S.W. Nam[d)], T. Saab,
B.A. Young[c)]

Physics Department, Stanford University, Stanford, CA 94305, USA

Abstract

We present evidence of an enhanced ballistic phonon component resulting from surface events in a 100 g silicon cryogenic dark matter detector. Surface events, calibrated using a ^{14}C electron source, were found to have faster rise times ($\sim 5\,\mu s$) than bulk gamma and neutron events ($\sim 7\mu s$). Using this effect, we were able to discriminate bulk nuclear recoil events from a surface electron background at better than the 97% level above 25 keV recoil energy. The phonon rise time for bulk gamma events was dependent on the applied voltage, confirming that phonons produced from electron-hole emission are ballistic.

0

a) Center for Particle Astrophysics, University of California, Berkeley, CA 94720

b) Fermi National Accelerator Laboratory, Batavia, IL 60510

c) Department of Physics, Santa Clara University, Santa Clara, CA 95053

d) National Institute of Standards and Technology, Boulder, CO 80303

By combining low temperature phonon measurements with conventional ionization measurement[1,2], large mass dark matter detectors for weakly interacting massive particles or WIMPs have been developed with a high degree of background rejection capability. The decreased ionization yield due to the nuclear recoil quenching factor[3] has enabled these detectors to discriminate between bulk gamma and nuclear recoil events at better than the 99% level[4]. Surface events, although they are not subject to nuclear quenching, produce fewer electron-hole (e-h) pairs than a photon of the equivalent recoil energy (E_r) which interacts deep within the crystal. The presence of this 'dead layer'[5] severely limits the ability of these detectors to discriminate between bulk nuclear recoils and a soft beta ($E_r \lesssim 100\,\mathrm{keV}$) background component. In addition, the charge noise in these large capacitance detectors limits our ability to discriminate gammas and neutrons at low threshold. A purely phonon-based technique would allow discrimination at lower recoil energies as we improve the sensitivity of the phonon measurement. Our experiments utilize a new generation cryogenic dark matter detector where the phonon sensors comprise 2 μm wide W Transition-Edge-Sensors (TES). They trap quasiparticles generated in attached Al fins[6]. This type of phonon sensor is intrinsically fast ($t_{rise} \simeq 5\,\mu$s, $t_{fall} \simeq 100\,\mu$s, phonon limited) and can image the event location in a 3 inch diameter crystal using phonon propagation delay (Fig.1a)[7].

The phonons that reach the sensor can be generated in a variety of ways. Particle interactions in silicon create primarily high frequency phonons that quickly undergo anharmonic decay ($\Gamma_D \propto \nu^5$), and diffuse due to isotopic scattering ($\Gamma_I \propto \nu^4$). The combination of the two scattering mechanisms creates a phenomenon known as quasi-diffusive transport[8]. Over microsecond timescales phonons approach an average frequency of ≈ 1 THz[9], and take longer than the ballistic time ($t \sim 3t_b$) to reach the surface of the detector. Phonons generated by e-h pairs drifting through the crystal due to the electric field of the ionization bias[10] are predicted to of be lower frequency[11] and thus travel ballistically. Previous estimates of the fraction of phonon energy propagating ballistically for electron recoils in silicon detectors[12] were small (~0.9%). Measurements of alpha induced phonons, however, indicated large ballistic components[13] (30%). Here we show that the discrepancy in these two estimates can be explained by the down conversion of phonons in the thin-film metals on the surface.

The detector consists of thin film metallic layers fabricated on a 10 mm thick 76 mm diameter crystal of high purity ($\rho > 8\,\mathrm{k\Omega}$-cm, uncompensated) silicon. The phonon side is covered (90%) with 150 nm thick Al patterned into collecting fins. Six fins, each with a length of 2 mm and a width of 40 μm, are connected to each W TES. Four separate phonon channels are instrumented (see inset Fig.1a) to allow the reconstruction of event location through phonon timing. Surrounding the phonon sensors is an outer perimeter of 25 nm thick W guard-electrode grid (10% area coverage, 20 μm spacing). The gap between the Al fins never exceeds 100 μm to ensure uniformity of the electric field required for the ionization measurement. The opposite face of the detector is the charge electrode and consists of a 20% area coverage grid (spacing 25 μm) of 5 nm/25 nm Ti/Au. [14].

When athermal phonons ($\mathrm{E}_{ph} > 2\Delta_{\mathrm{Al}}$) from a particle event reach the surface of the detector, they inelastically scatter in the Al fins and generate quasiparticles. These quasiparticles then diffuse into 444 tungsten TES elements, connected in parallel, that are voltage biased within their superconducting transition (T_c=65 mK). The resulting current pulse is read out by a high-bandwidth (>1 MHz) SQUID array[15]. All processes involved are intrinsically faster than the phonon transit times with the exception of the quasiparticle trapping time, estimated to be $\approx 3\,\mu$s. For the ionization measurement a bias voltage of approximately 1 V is applied between the phonon side (always ground) and charge side of the detector. The ionization signal is read out by a conventional charge sensitive amplifier.

A ^{14}C electron source was mounted on the ionization readout side of the detector 10 mm from the surface. Four collimator holes, 25 mm apart, produced a combined rate of 100 Hz and spot sizes on the surface $\sim$3 mm in diameter. An ^{241}Am source was mounted on the opposite side (phonon side, see inset Fig.1b) to provide 60 keV photons. The detector was cooled to 30 mK using an Oxford Instruments 75 μW dilution refrigerator. Phonon and ionization pulses were digitized at 10 MHz with a total record length of 1 ms.

By comparing the delay between the 4 phonon sensors (CD-AB) vs. (BC-AD), the 4 collimated spots from the electron source were easily separated from the uniform background (see Fig.1a)). Figure 1b shows the scatter distribution of electrons at 5 μs rise time with a recoil spectrum consistent with the allowed beta spectrum of ^{14}C. The 60 keV photons showed a rise time distribution peaked at 7.5 μs with a 1σ width of 0.75 μs. A tail in the 60 keV photon distribution extends to low rise time and low charge collection ($y \equiv n_{eh}/\mathrm{E}_r$). These events can be attributed to photons interacting close to the (charge side) surface. This feature enabled us to estimate the characteristic length scale of $\sim$300 μm for the rise time enhancement depth. To explain this effect we construct a simple model where initial phonons interact in the metallic surface layer (25 nm Au grid) and heat it locally to above 1K. The metal then reradiates phonons according to a Plank distribution[16], which travel ballistically across the detector. This model gives a distance scale of $\sim$100 μm where the local energy density is high enough to heat the gold layer to 1K, in reasonable agreement with our measured value.

In another experiment we measured the nuclear recoil response of the detector using a ^{252}Cf neutron source placed 0.5 m from the cryostat. This response is important for dark matter detectors since supersymmetric WIMP candidates will deposit energy primarily through elastic nuclear scattering[17]. Figure 2a shows the ability of the detector to separate neutron, gamma and beta events at 50-70 keV (chosen to include the 60 keV gammas). Electrons and neutrons both appear with low y but are separated using the phonon rise time. To separate the charge-based (y) discrimination from rise time we performed a cut in y (shown as the vertical dotted lines in Figure 2a. We then define in the usual way[18] a quality factor, $Q = (\beta(1-\beta))/(\alpha-\beta)^2$, where β is the fraction of background events (electrons) and α is the fraction of signal events (neutrons) that survive. The quantity Q gives the fractional reduction in the signal upper limit as $\sqrt{Q/MT}$ after performing statistical background subtraction (M≡mass,T≡time). The variation of Q with rise time (cut position) is shown in Figure 2b(inset)) for 50-70 keV. The minimum of Q is plotted as a function of energy in Figure 2b. The rise in Q at low energy is caused by detector noise.

In a final experiment the bias voltage across the detector for the ionization measurement was varied from 0 to 3 volts. This range caused the fraction of phonons, shed by e-h pairs, to increase from zero to 44% (a correction for charge collection efficiency was applied) and the rise time of the 60 keV signal to decrease from ~8 μs to ~6.5μs (Fig.3). With a simple model for our detector response we were able to simulate this effect using two populations of phonons. The first population arrives with a 8.6 μs characteristic fall time (30% absorption at the phonon detector, ballistic velocity) and the other with a 25.8 μs fall time (consistent with $v \sim \frac{v_b}{3}$). The detector was modelled using two single pole filters of 2.5 μs for the quasiparticle relaxation time and 10 μs for the ETF response time[14]. A difference in frequency between intrinsic phonons and those shed by e-h pairs may, in the future, be used to discriminate between bulk gammas and neutrons without the limitations of an ionization readout.

In these series of experiments we have demonstrated the ability to use phonon rise time to discriminate between bulk nuclear and surface electron events. Likely, the effect is caused by the downconversion of high frequency phonons in the metal thin-films at the detector surfaces. The variation of rise time with applied voltage points strongly to the generation of ballistic phonons by drifting electron-hole pairs, which may prove useful in future phonon-based discrimination schemes.

This work was supported in part by the Department of Energy under contracts DE-FG03-90ER40569, DE-FG03-91ER40618 and DE-AC03-76SF00098, by the Center for Particle Astrophysics (an NSF Science and Technology Center operated by UC Berkeley) under Cooperative Agreement No. AST-91-20005. We gratefully acknowledge the skillful and dedicated efforts of the technical staffs at FermiLab, LBNL, Stanford University, UC Berkeley, and UC Santa Barbara.

REFERENCES

[1] N.E. Booth, B. Cabrera and E. Fiorini, *Ann. Rev. Nucl. Part. Sci.* **46**, 471 (1996).

[2] D. Yvon, N. Wang, M. Chapellier, G. Chardin, P. Leveque, D. LHote, P. Pari, J. Soudee and G. Guerrier, *J. Low Temp. Phys.* **93**, 405 (1993).

[3] J. Lindhard, V. Nielsen, M. Scharff and P.V. Thomsen,*Mat. Fys. Medd. Dan. Selk.* **33**, 10 (1963). B.L. Dougherty, *Phys. Rev.* A **45**, 2104 (1992).

[4] T. Shutt, N. Wang, B. Ellman, Y. Giraud-Heraud, C. Stubbs, P.D. Barnes Jr., A. Cummings, A. Da Silva, J. Emes, E.E. Haller, A.E. Lange, J. Rich, R.R. Ross, B. Sadoulet, G. Smith, W. Stockwell, S. White, B.A. Young and D. Yvon, *Phys. Rev. Lett.* **69**, 3531 (1992).

[5] T. Shutt, M. Cunningham, A. DaSilva, R. Diaz, J. Emes, R.J. Gaitskell, S.R. Golwala, E.E. Haller, J. Jochum, R.R. Ross, B. Sadoulet, D. Seitz, G. Smith, A. Sonnenschein, R. Therrien and S. White, *Proc. Seventh Int. Workshop on Low Temp Det. (LTD-7)*, ed. S. Cooper, 224 (1997).

[6] K.D. Irwin, *Appl. Phys. Lett.* **66**, 1998 (1995). S.W. Nam, B. Cabrera, R.M. Clarke, C. Fertig, K.D. Irwin and B.A. Young, *Nucl. Instrum. Methods* A **370**, 187 (1996).

[7] P.L. Brink, B. Cabrera, B. Chugg, R.M. Clarke, A. Davies, S.W. Nam, and B.A. Young, *Czech. J. Phys.* **46**, 2887 (1996). B. Cabrera, P. L. Brink, B. Chugg, R. M. Clarke, A. K. Davies, S. W. Nam, and B. A. Young, *The Identification of Dark Matter*, ed. N. J. C. Spooner, pp. 353-361 (World Scientific, 1997).

[8] Y.B. Levinson, *Nonequilibrium Phonons in Nonmetallic Crystals*, eds. W. Eisenmenger and A.A. Kaplyanskii, p. 91. (Elsevier, 1986).

[9] S. Tamura, *Phys. Rev.* B **56**, 13630 (1997).

[10] B. Neganov and V. Trafimov, Otkrytia: Izobreteniya **146**, 215 (1985). P.N. Luke, *J. Appl. Phys.* **64**, 6858 (1988).

[11] B. Cabrera, B.L. Dougherty, A.T. Lee, M.J. Penn, J.G. Pronko and B.A. Young, *J. Low Temp. Phys.* **93**, 365 (1993).

[12] A.T. Lee, B. Cabrera, B.L. Dougherty, M.J. Penn, J.G. Pronko and S. Tamura, *Phys. Rev.* B **54**, 3244 (1996).

[13] B.A. Young, B. Cabrera and A.T. Lee, *Phys. Rev. Lett.* **64**, 2795 (1990).

[14] R.M. Clarke, P.L. Brink, S.W. Nam, A.K. Davies, B. Chugg, B.A. Young and B. Cabrera, *Proc. Seventh Int. Workshop on Low Temp Det. (LTD-7)*, ed. S. Cooper, 229 (1997).

[15] R.P. Welty and J.P. Martinis, *IEEE Trans. Appl. Supercon.* **3**, 2605 (1993).

[16] See references in *Imaging Phonons: Acoustic Wave propagation in Solids*, J. P. Wolfe, (Cambridge University Press, 1998).

[17] G. Jungman, M. Kamionkowski and K. Griest, *Phys. Rep.* **267**, 196 (1996).

[18] P.F. Smith and J.D. Lewin, *Astroparticle Physics* **6**, 87 (1996). R.J. Gaitskell, P. D. Barnes Jr., A. DaSilva, B. Sadoulet, and T. Shutt, *Nucl. Phys.* B *Proc.Suppl.* **51**, 279 (1996).

FIGURES

FIG. 1. (a) Phonon delay in X (CD-AB) vs. delay in Y (BC-AD) for 60 keV. Inset: The four phonon sensor geometry. The four collimated distributions from the ^{14}C source are clearly visible above the uniform background (r $\sim 15\,\mu$s). The ^{241}Am source forms two spots (obscured by the electrons) on the x-axis. (b) Phonon rise time vs. phonon energy for events near zero X or Y delay (see a). Inset: Detector and source geometry.

FIG. 2. (a) Phonon rise time (t_r) vs. charge yield (y) for 50-70 keV recoil energy. Electrons form a distribution on the lower left (low y and fast t_r), Neutrons upper left (low y and slow t_r), and gammas (large y) upper right. Dotted lines are used to define a quality factor (Q) for pure y and t_r discrimination. (b) Optimal Q vs. t_r vs. energy with 90% confidence (crosses). Horizontal bars depict the energy range of calculation. Inset: Q vs t_r for 50-70 keV with 90% confidence (dotted), and $\frac{\beta}{\alpha}$ vs. t_r (faint line).

FIG. 3. A plot of phonon rise time for 60 keV photons vs. the fraction of phonon signal produced by drifting e-h pairs (circles); The model prediction (crosses). Inset: Rise time distributions for 0.1 volts and 3 volts (10% and 44%) with gaussian fits (solid line).

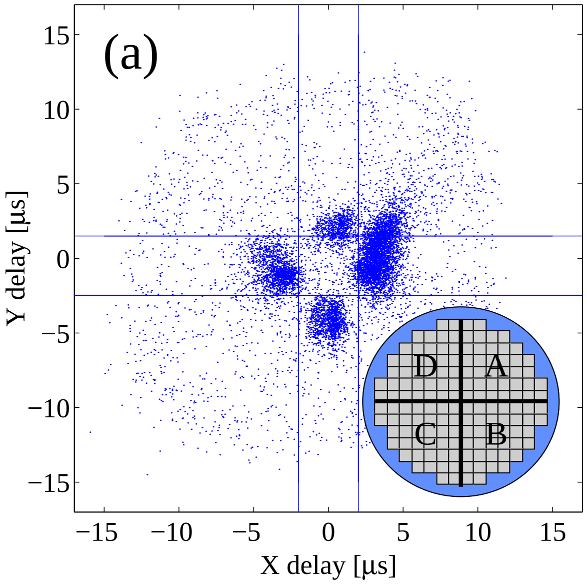
(a)
Y delay [µs]
X delay [µs]
15
10
5
0
−5
−10
−15
−15
−10
−5
0
5
10
15
D
A
C
B

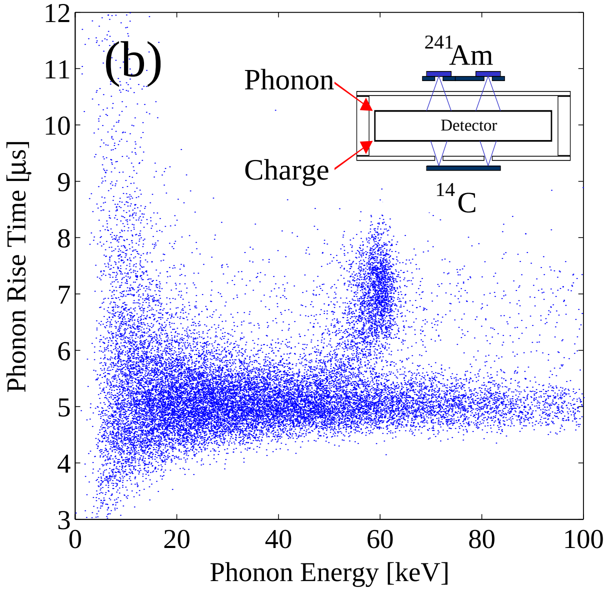
(b)
^{241}Am
Phonon
Detector
Charge
^{14}C
Phonon Rise Time [µs]
Phonon Energy [keV]
12
11
10
9
8
7
6
5
4
3
0
20
40
60
80
100

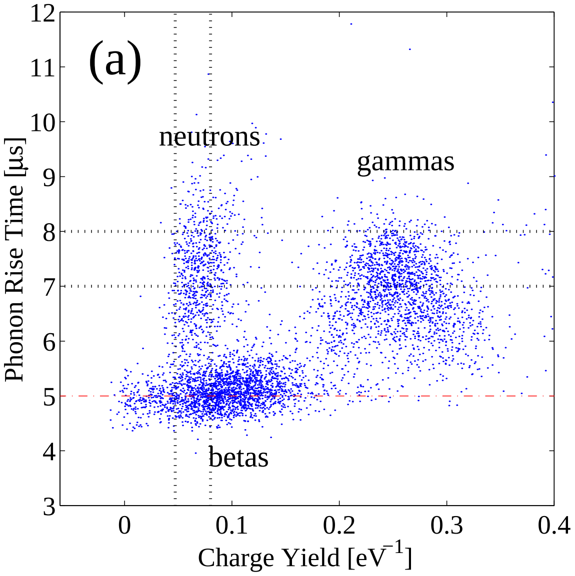
(a)
neutrons
gammas
betas
Phonon Rise Time [µs]
Charge Yield [eV^{-1}]
3
4
5
6
7
8
9
10
11
12
0
0.1
0.2
0.3
0.4

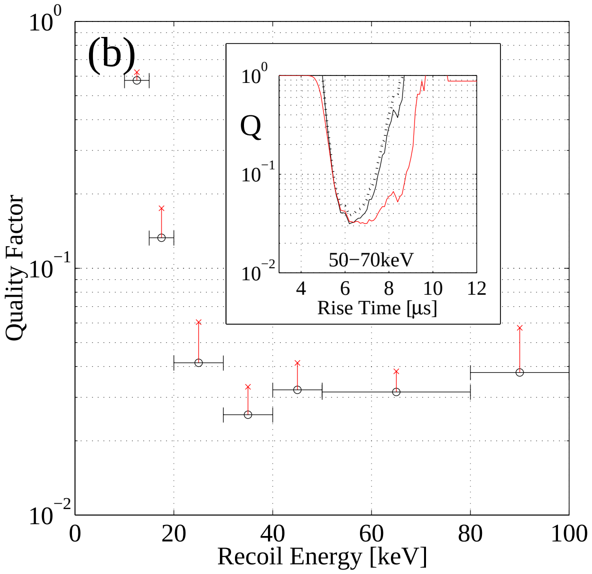
(b)
Quality Factor
Recoil Energy [keV]
10^0
10^{-1}
10^{-2}
0
20
40
60
80
100
Q
50−70keV
Rise Time [µs]
4
6
8
10
12

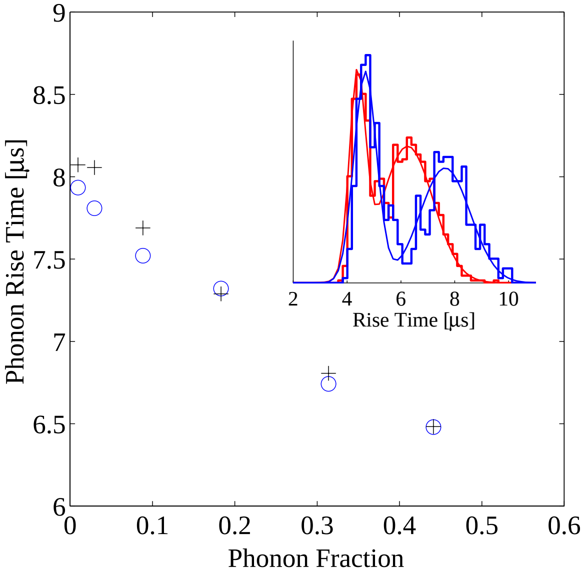
Phonon Rise Time [µs]
9
8.5
8
7.5
7
6.5
6
0
0.1
0.2
0.3
0.4
0.5
0.6
Phonon Fraction
2
4
6
8
10
Rise Time [µs]